

Oocyte formation by mitotically active germ cells purified from ovaries of reproductive-age women

Yvonne A R White^{1,2,4}, Dori C Woods^{1,2,4}, Yasushi Takai³, Osamu Ishihara³, Hiroyuki Seki³ & Jonathan L Tilly^{1,2}

Germline stem cells that produce oocytes *in vitro* and fertilization-competent eggs *in vivo* have been identified in and isolated from adult mouse ovaries. Here we describe and validate a fluorescence-activated cell sorting-based protocol that can be used with adult mouse ovaries and human ovarian cortical tissue to purify rare mitotically active cells that have a gene expression profile that is consistent with primitive germ cells. Once established *in vitro*, these cells can be expanded for months and can spontaneously generate 35- to 50- μ m oocytes, as determined by morphology, gene expression and haploid (1n) status. Injection of the human germline cells, engineered to stably express GFP, into human ovarian cortical biopsies leads to formation of follicles containing GFP-positive oocytes 1–2 weeks after xenotransplantation into immunodeficient female mice. Thus, ovaries of reproductive-age women, similar to adult mice, possess rare mitotically active germ cells that can be propagated *in vitro* as well as generate oocytes *in vitro* and *in vivo*.

Since the early 1950s, management of ovarian insufficiency and failure, including infertility caused by aging or insults, was restricted by the belief that the oocyte-containing pool of follicles set forth at birth is not amenable to renewal¹. In 2004, studies with mice challenged the idea of a fixed ovarian reserve being endowed during the perinatal period². Based on results from several approaches, it was concluded that the ovaries of adult mice possess rare female germline or oogonial stem cells (OSCs) that generate oocytes in a way analogous to the spermatogonial stem cell support of sperm production in adult testes³. Although this previous study was criticized by many in the field⁴, several years later OSCs were successfully isolated from neonatal and adult mouse ovaries. The cells were shown to stably proliferate *in vitro* for months^{5,6} and spontaneously generate what seem to be immature oocytes in culture⁶. Transplantation studies showed that GFP-expressing mouse OSCs injected into ovaries of chemotherapy-conditioned adult mice differentiate into mature eggs that are ovulated, fertilize and produce viable offspring⁵. These findings, along with other studies of mice^{7–9}, have opened the possibility of using OSCs as agents for transplantation and targets for therapies designed to modulate ovarian function and fertility^{4,10}. Additionally, identification of dormant OSCs in atrophic ovaries of aged mice, which resume *in vivo* oogenesis when exposed to a young-adult (2 months of age) ovarian environment¹¹, indicates that ovarian aging may be reversible^{10,12}. However, any consideration of a possible clinical utility of these cells requires firm evidence that comparable oocyte-producing cells exist in ovaries of reproductive-age women.

As a first step toward this goal, we critically assessed a recently reported protocol to obtain OSCs from adult mouse ovaries⁵. This approach relies on the immunological detection of a putative cell-surface variant of Ddx4 (DEAD box polypeptide 4, also commonly

referred to as mouse vasa homolog or Mvh), an evolutionarily conserved germ-cell-specific RNA helicase^{13–15}, coupled with cell sorting using magnetic beads. Two issues surfaced that we felt might preclude application of this protocol to isolate candidate OSCs from adult human ovaries. First, Ddx4 is widely considered to be a cytoplasmic protein and, thus, its reported detection on the surface of mouse OSCs is at odds with the results from prior studies^{10,16}. Second, even if a cell-surface variant of Ddx4 is expressed by mouse OSCs, immunomagnetic sorting is a relatively crude approach to cell isolation that often results in the enrichment of a desired cell type in fractions that are contaminated with non-targeted cells carried over during the column washing and flushing steps. Magnetic bead sorting also does not distinguish between viable and damaged or dead cells and does not allow for simultaneous assessment of other cellular features, such as yield, size or co-expression of additional markers. Our objectives were to initially test with mice whether or not OSCs possess an externally exposed epitope of Ddx4 and, if so, to use this property for validation of a fluorescence-activated cell sorting (FACS)-based protocol to purify viable OSCs from the dispersed ovaries of adult mice. We next determined whether this technology could also be used to purify an equivalent population of candidate OSCs from the ovarian cortical tissue of healthy reproductive-age women. Once we isolated mouse and human OSCs by FACS, we then tested their growth properties and functionality using both *in vitro* and *in vivo* approaches.

RESULTS

Validation of a FACS-based protocol for OSC isolation

The antibody to Ddx4 used previously to isolate mouse OSCs by immunomagnetic sorting is a rabbit polyclonal antibody against the

¹Vincent Center for Reproductive Biology, Massachusetts General Hospital Vincent Department of Obstetrics and Gynecology, Massachusetts General Hospital, Boston, Massachusetts, USA. ²Department of Obstetrics, Gynecology and Reproductive Biology, Harvard Medical School, Boston, Massachusetts, USA.

³Department of Obstetrics and Gynecology, Saitama Medical Center, Saitama Medical University, Saitama, Japan. ⁴These authors contributed equally to this work. Correspondence should be addressed to J.L.T. (jtilly@partners.org).

Received 26 August 2011; accepted 11 January 2012; published online 26 February 2012; doi:10.1038/nm.2669

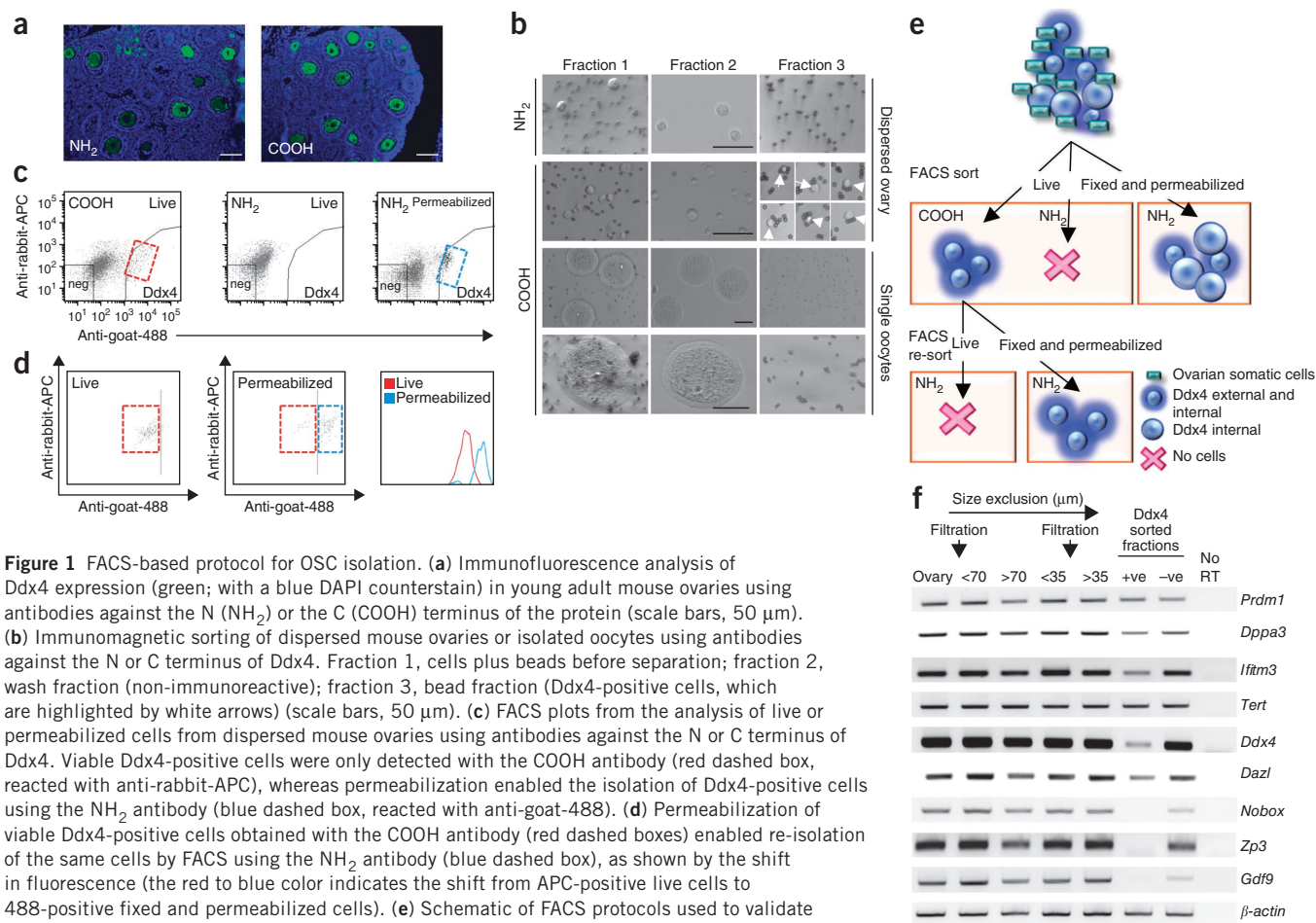


Figure 1 FACS-based protocol for OSC isolation. **(a)** Immunofluorescence analysis of Ddx4 expression (green; with a blue DAPI counterstain) in young adult mouse ovaries using antibodies against the N (NH₂) or the C (COOH) terminus of the protein (scale bars, 50 μ m). **(b)** Immunomagnetic sorting of dispersed mouse ovaries or isolated oocytes using antibodies against the N or C terminus of Ddx4. Fraction 1, cells plus beads before separation; fraction 2, wash fraction (non-immunoreactive); fraction 3, bead fraction (Ddx4-positive cells, which are highlighted by white arrows) (scale bars, 50 μ m). **(c)** FACS plots from the analysis of live or permeabilized cells from dispersed mouse ovaries using antibodies against the N or C terminus of Ddx4. Viable Ddx4-positive cells were only detected with the COOH antibody (red dashed box, reacted with anti-rabbit-APC), whereas permeabilization enabled the isolation of Ddx4-positive cells using the NH₂ antibody (blue dashed box, reacted with anti-goat-488). **(d)** Permeabilization of viable Ddx4-positive cells obtained with the COOH antibody (red dashed boxes) enabled re-isolation of the same cells by FACS using the NH₂ antibody (blue dashed box), as shown by the shift in fluorescence (the red to blue color indicates the shift from APC-positive live cells to 488-positive fixed and permeabilized cells). **(e)** Schematic of FACS protocols used to validate the Ddx4 COOH antibody for the isolation of viable OSCs. **(f)** Expression analysis of germline markers (*Prdm1*, *Dppa3*, *Ifitm3*, *Tert*, *Ddx4* and *Dazl*) and oocyte markers (*Nobox*, *Zp3* and *Gdf9*) in each cell fraction produced during the ovarian dispersion process to obtain cells for FACS-based isolation of OSCs. +ve, Ddx4-positive viable cell fraction after FACS; -ve, Ddx4-negative viable cell fraction after FACS; no RT, PCR of RNA sample without reverse transcription; β -actin, sample loading control. Samples were resolved through agarose gels and stained with ethidium bromide to visualize DNA bands, with the resultant images inverted for photography and display purposes.

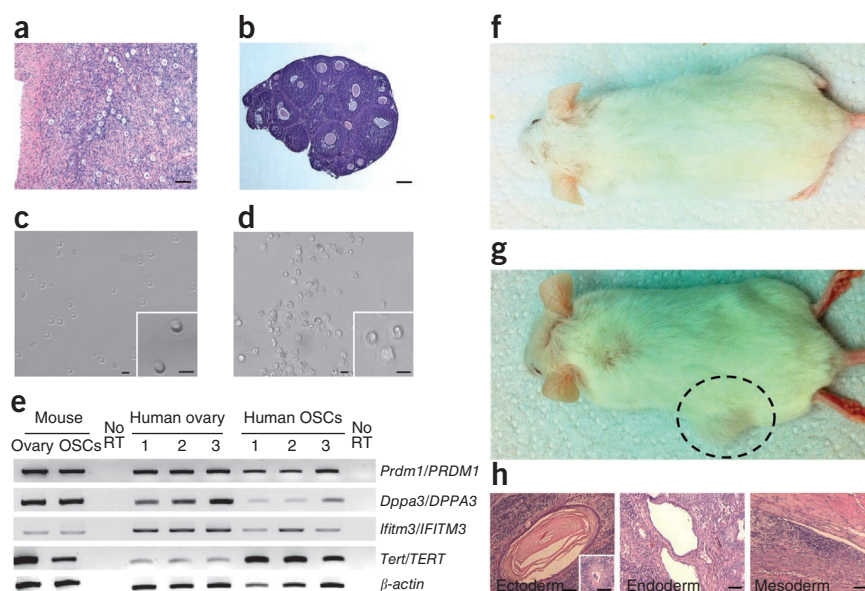
C terminus of the protein (hereafter called the COOH antibody)⁵. We obtained this antibody, along with a goat polyclonal antibody against the N terminus of Ddx4 (hereafter called the NH₂ antibody), for our comparative studies. An immunofluorescence analysis of ovaries from young-adult mice using either of the two antibodies showed an identical pattern of Ddx4 expression that was restricted to the oocytes (Fig. 1a). We then used each antibody for immunomagnetic sorting of dispersed ovary tissue from young-adult mice⁵. We obtained no cells in the bead fraction when we used the NH₂ antibody; however, we observed 5- to 8- μ m cells bound to the magnetic beads when we used the COOH antibody (Fig. 1b). An analysis of the cells isolated with the COOH antibody revealed a germline gene expression pattern consistent with that previously reported for mouse OSCs isolated using immunomagnetic sorting⁵ (Supplementary Fig. 1). Although we always detected the isolated oocytes in the non-immunoreactive wash fraction using the COOH antibody when assessed in parallel (Fig. 1b), a more thorough marker analysis of the Ddx4-positive viable cell fraction obtained by immunomagnetic sorting revealed several oocyte-specific mRNAs, including mRNA of the *Nobox* (new-born ovary homeobox), *Zp3* (zona pellucida glycoprotein 3) and *Gdf9* (growth differentiation factor 9) genes (Supplementary Fig. 1). These findings indicate that although mouse oocytes do not show evidence of cell-surface expression of Ddx4 when analyzed as individual

entities (Fig. 1b), mouse oocytes are nonetheless a contaminating cell type after immunomagnetic sorting of OSCs from dispersed mouse ovary tissue. This outcome probably reflects either a non-specific physical carryover of small oocytes with OSCs during column washing and flushing or a reactivity of cytoplasmic Ddx4 in plasma-membrane-compromised (damaged) oocytes with the COOH antibody.

Therefore, we next tested the reactivity of each of the two antibodies with dispersed mouse ovarian cells by FACS. In agreement with the results from the magnetic bead sorting, we only obtained viable Ddx4-positive cells when we used the COOH antibody (Fig. 1c). However, if we fixed and permeabilized the ovarian cells before FACS, we also obtained Ddx4-positive cells using the NH₂ antibody (Fig. 1c). Furthermore, if we fixed, permeabilized and re-sorted the viable Ddx4-positive cells that we isolated by FACS using the COOH antibody, the same cell population was also recognized by the NH₂ antibody (Fig. 1d). As a final means to confirm the validity of this OSC isolation method (Fig. 1e), we assessed the fractions of cells obtained at each step of the protocol by gene expression analysis using the following markers for germ cells: *Prdm1* (PR domain containing 1 with ZNF domain, which has the human gene ortholog *PRDM1*, also commonly referred to as *BLIMP1*), *Dppa3* (developmental pluripotency-associated 3, with the human gene ortholog *DPPA3*, also commonly referred to as *STELLA*), *Ifitm3* (interferon induced

Figure 2 Isolation of OSCs from adult mouse

and human ovaries. (a,b) Representative histological appearance of adult ovarian tissue used for the isolation of human (a) and mouse (b) OSCs. Scale bars, 100 μ m. (c,d) Morphology of viable cells isolated by FACS based on cell-surface expression of DDX4 (human, left) or Ddx4 (mouse, right). Scale bars, 10 μ m; insets show a twofold higher magnification of individual OSCs. (e) Gene expression profile of the starting ovarian material and freshly isolated OSCs showing an assessment of three different subjects as examples for the human ovarian tissue analyses. Samples were resolved through agarose gels and stained with ethidium bromide to visualize DNA bands, with the resultant images inverted for photography and display purposes. (f,g) Teratoma formation assay showing an absence of tumors in NOD-SCID mice 24 weeks after receiving injections of freshly isolated mouse OSCs (f) compared with development of tumors in mice 3 weeks after the injection of an equivalent number of mouse ESCs (g; with the tumor highlighted by a black-dashed oval). (h) Examples of cells from all three germ layers in a representative ESC-derived teratoma, with a neural rosette highlighted at the same magnification in the inset of the left panel (scale bars, 100 μ m).



transmembrane protein 3, also commonly referred to as *Fragilis*, with the human gene ortholog *IFITM3*), *Tert* (telomerase reverse transcriptase, with the human gene ortholog *TERT*), *Ddx4* (with the human gene ortholog *DDX4*) and *Dazl* (deleted in azoospermia-like, with the human gene ortholog *DAZL*). For oocytes, we used the markers *Nobox*, *Zp3* and *Gdf9*. We minced and enzymatically digested adult mouse ovarian tissue and passed it through a 70- μ m filter to remove large tissue clumps and then through a 35- μ m filter to obtain the final fraction of cells for FACS. Every fraction of cells in each step of the protocol, with the exception of the Ddx4-positive viable cell fraction obtained by FACS, expressed all germline and oocyte markers (Fig. 1f). Although FACS-sorted Ddx4-positive cells expressed all germline markers, we detected no oocyte markers in these cells (Fig. 1f). Thus, unlike the oocyte contamination observed when we isolated OSCs by immunomagnetic sorting using the Ddx4 COOH antibody (Supplementary Fig. 1), use of this antibody with FACS provided a strategy to obtain OSCs free of oocytes.

FACS isolation of candidate OSCs from adult human ovaries

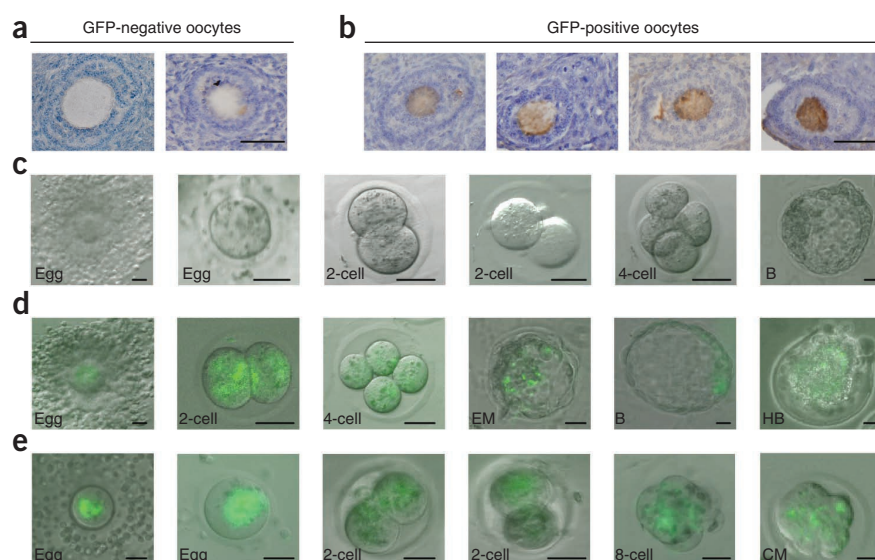
Using the COOH antibody with FACS, we consistently isolated viable DDX4-positive cells of 5–8 μ m in diameter from human ovarian cortical tissue of all subjects analyzed ($n = 6$), with a percent yield ($1.7\% \pm 0.6\%$ (mean \pm s.e.m.) DDX4-positive as compared to the total viable cells sorted) that was comparable to the yield of OSCs from young-adult mouse ovaries that we processed in parallel ($1.5\% \pm 0.2\%$ Ddx4-positive compared to the total viable cells sorted; $n = 15$). The percent yield is the incidence of Ddx4-positive cells in the final pool of viable single cells sorted by FACS, which represents only a fraction of the total number of cells present in the ovaries before processing. To estimate the incidence of OSCs per ovary, we used young-adult mice to determine the genomic DNA content per ovary ($1,774.44 \mu\text{g} \pm 426.15 \mu\text{g}$ (mean \pm s.e.m.); $n = 10$) and divided this value into the genomic DNA content per fraction of viable cells sorted per ovary ($16.41 \mu\text{g} \pm 4.01 \mu\text{g}$; $n = 10$). Assuming the genomic DNA content per cell in these mice is equivalent, this allowed us to determine how much of the total ovarian cell pool was represented by the total viable

sorted cell fraction obtained after processing. Using this correction factor, we estimated the incidence of OSCs per ovary in the mice to be $0.014\% \pm 0.002\%$ ($0.00926 \times (1.5\% \pm 0.2\%)$). The OSC yield varied across multiple replicates, but we consistently obtained between 250 to slightly over 1,000 viable Ddx4-positive cells from each young-adult mouse ovary after FACS of dispersates that we initially prepared from a pool of four young-adult mouse ovaries.

Analyses of freshly isolated Ddx4- and DDX4-positive cells from mouse and human ovaries, respectively, (Fig. 2a,b) revealed similar sizes and morphology between the mouse and human cells (Fig. 2c,d), as well as matched gene expression profiles rich in markers for early germ cells^{17–19} (the markers *Prdm1* and *PRDM1*, *Dppa3* and *DPPA3*, *Ifitm3* and *IFITM3*, and *Tert* and *TERT* for mice and humans, respectively; Fig. 2e). These findings agree with the previously reported morphology and gene expression profile of mouse OSCs^{5,6}. To further define characteristic features of Ddx4-positive cells obtained from adult ovaries using FACS, we first performed an *in vivo* teratoma formation assay. We felt this was a crucial step, as a recent study reported the isolation of stem cells positive for Pou5f1 (POU domain class 5 transcription factor 1) from adult mouse ovaries that possess the teratoma-forming capacity of embryonic stem cells (ESCs) and induced pluripotent stem cells²⁰. All (100%) of the nonobese diabetic (NOD)-severe combined immunodeficient (SCID) mice we transplanted with 1×10^5 mouse ESCs that we used as positive controls ($n = 3$) developed teratomas within 3 weeks of transplantation; however, we observed no teratomas in NOD-SCID mice that we transplanted in parallel with 1×10^5 Ddx4-positive cells freshly isolated from adult mouse ovaries ($n = 3$), even at 24 weeks after transplantation (Fig. 2f–h). Thus, although OSCs express numerous stem cell and primitive germ cell markers^{5,6} (Figs. 1f and 2e), these cells are distinct from the other types of pluripotent stem cells that have previously been described.

We next engineered FACS-purified mouse OSCs to express GFP using retroviral transduction after we established the cells as actively dividing germ-cell-only cultures *in vitro* (see below). We then used these cells to test the ability of mouse OSCs to generate oocytes after

Figure 3 Mouse OSCs generate functional eggs after intraovarian transplantation. (a,b) Examples of growing follicles containing GFP-negative (a) and GFP-positive (b) (brown; with a blue hematoxylin counterstain) oocytes in ovaries of wild-type mice injected with GFP-expressing OSCs 5–6 months before analysis. (c) Examples of ovulated GFP-negative eggs (in cumulus-oocyte complexes) and the resultant embryos (embryos at the two-cell (2-cell), four-cell (4-cell), and blastocyst (B) stages are shown as examples) generated by IVF after induced ovulation of wild-type female mice that received intraovarian transplantation of GFP-expressing OSCs 5–6 months before analysis. Scale bars, 30 μ m. (d,e) Examples of GFP-positive eggs (in cumulus-oocyte complexes) obtained from the oviducts after induced ovulation of wild-type female mice that received intraovarian transplantation of GFP-expressing OSCs 5–6 months before analysis. These eggs were fertilized *in vitro* using wild-type sperm, resulting in two-cell embryos that progressed through preimplantation development (examples of GFP-positive embryos at the two-cell, four-cell, eight-cell (8-cell), compacted morula (CM), expanded morula (EM), blastocyst and hatching blastocyst (HB) stages are shown) to form hatching blastocysts 5–6 d after fertilization. Scale bars, 30 μ m.



transplantation into the ovaries of adult female mice. To ensure that the outcomes we obtained were reflective of the stable integration of the transplanted cells into the ovaries and also that the outcomes were not complicated by pre-transplantation-induced damage to the gonads, we injected GFP-expressing mouse OSCs into ovaries of non-chemotherapy-conditioned wild-type recipient mice at 2 months of age, and we maintained the mice for 5–6 months before analysis. At between 7 and 8 months of age, we induced the transplanted mice to ovulate using exogenous gonadotropins, after which we collected their ovaries and any oocytes released into the oviducts. We readily detected developing follicles containing GFP-positive oocytes, along with host follicles containing GFP-negative oocytes, in ovaries of all female mice that received GFP-expressing mouse OSCs that were initially purified by FACS (Fig. 3a,b).

After oviductal flushing, we observed complexes containing expanded cumulus cells surrounding centrally located oocytes both lacking and expressing GFP. Mixing these complexes with sperm from wild-type male mice resulted in fertilization and the development of preimplantation embryos, with those embryos that were derived from fertilized GFP-positive eggs retaining GFP expression through the hatching blastocyst stage (Fig. 3c–e). From the five adult wild-type female mice transplanted with GFP-expressing OSCs 5–6 months before evaluation, we retrieved a total of 31 cumulus-oocyte complexes from the oviducts, 23 of which successfully fertilized to produce embryos. The presence of cumulus cells around each oocyte made it impossible for us to accurately determine the number of GFP-negative as compared to GFP-positive oocytes ovulated. However, an evaluation of the 23 embryos produced after *in vitro* fertilization (IVF) revealed that eight were GFP positive, with all five mice tested releasing at least one egg at ovulation that fertilized to produce a GFP-positive embryo. These findings indicate that mouse OSCs purified by FACS using the DDX4 COOH antibody, like their previously reported counterparts isolated from mouse ovaries by immunomagnetic sorting using the same antibody⁵, generate functional oocytes *in vivo*. However, our data also show that chemotherapy conditioning before transplantation is not, as previously reported⁵, required for OSCs to engraft and generate functional oocytes in adult mouse ovary tissue.

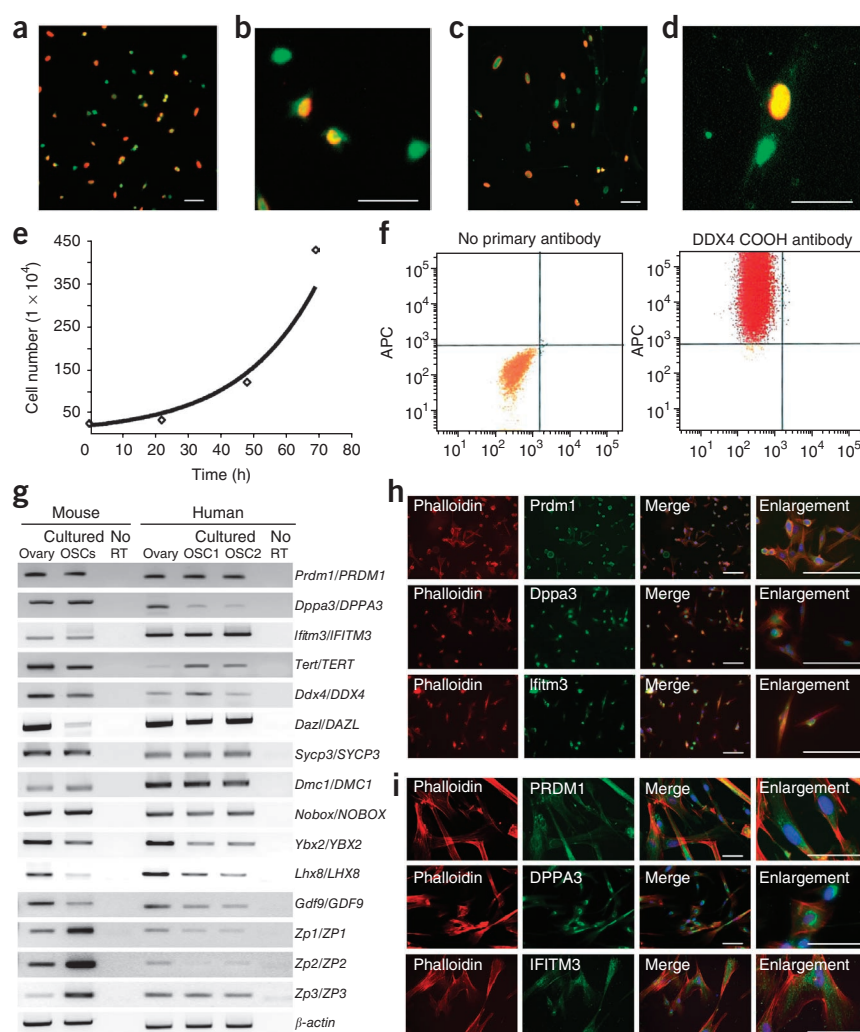
***In vitro* characterization of candidate human OSCs**

Using parameters described previously for the *in vitro* propagation of mouse OSCs⁵, we placed adult mouse-ovary-derived Ddx4-positive cells and adult human-ovary-derived DDX4-positive cells into defined cultures with mitotically inactive mouse embryonic fibroblasts (MEFs) as feeders. We could establish freshly isolated OSCs as clonal cell lines, and the colony formation efficiency for human OSCs not seeded onto MEFs ranged from 0.18–0.40%. We could not perform an accurate assessment of colony formation efficiency by OSCs using MEFs as initial feeders, the latter of which greatly facilitate the establishment of mouse and human OSCs *in vitro*. After 10–12 weeks (mouse) or 4–8 weeks (human) in culture, actively dividing germ-cell colonies became readily apparent (Supplementary Fig. 2). Once the OSCs were established and proliferating, the cells could be reestablished as germ-cell-only cultures in the absence of MEFs without loss of proliferative potential. A dual analysis of Ddx4 or DDX4 expression and bromodeoxyuridine (BrdU) incorporation in MEF-free cultures of mouse or human OSCs, respectively, revealed large numbers of cells double positive for Ddx4 (mouse) or DDX4 (human) and BrdU (Fig. 4a–d). These data confirmed that the adult mouse- and human-ovary-derived OSCs were actively dividing. At this stage, the mouse cells required passage at confluence every 4–5 d, with the cultures being split 1:6 or 1:8 (with an estimated doubling time of 14 h; Fig. 4e). The rate of mouse OSC proliferation was approximately two-fold to threefold higher than that of the human OSCs maintained in parallel, the latter of which required passage at confluence every 7 d, with cultures being split at either 1:3 or 1:4.

Cell-surface expression of Ddx4 was detectable on the surface of more than 95% of the OSCs after 18 months of propagation (Fig. 4f). The remaining cells not positive for cell-surface expression of Ddx4 after FACS using the COOH antibody were large (up to 35 μ m in diameter, with any cells >35 μ m excluded prior to FACS by filtration) spherical cells spontaneously produced by OSCs during culture, which showed cytoplasmic expression of Ddx4 and will be described in detail in the next section. A gene expression analysis of the cultured cells confirmed maintenance of early germline markers (Fig. 4g). We also detected several oocyte-specific markers in these cultures,

Figure 4 Evaluation of mouse- and human-ovary-derived OSCs in defined cultures.

(a–d) Assessment of OSC proliferation by dual detection of Ddx4 or DDX4 expression (green) and BrdU incorporation (red) in mouse (a,b) and human (c,d) OSCs maintained in MEF-free cultures. Scale bars, 30 μ m. (e) Typical growth curve for MEF-free cultures of mouse OSCs after passage and after seeding 2.5×10^4 cells in each well of 24-well culture plates. (f) FACS analysis using the COOH antibody to detect cell-surface expression of Ddx4 in mouse OSCs after 18 months of propagation. (g) Gene expression profile of starting ovarian material and cultured mouse and human OSCs after 4 or more months of propagation *in vitro*. Two different human OSC lines (OSC1 and OSC2) that were established from the ovaries of two different subjects are shown as examples. Samples were resolved through agarose gels and stained with ethidium bromide to visualize DNA bands, with the resultant images inverted for photography and display purposes. (h,i) Immunofluorescence analysis of Prdm1 and PRDM1, Dppa3 and DPPA3, and Ifitm3 and IFITM3 expression (green) in mouse (h) and human (i) OSCs in MEF-free cultures. Cells were counterstained with DAPI (blue) and rhodamine-phalloidin (red) to visualize nuclear DNA and cytoplasmic F-actin, respectively. Scale bars, 50 μ m.



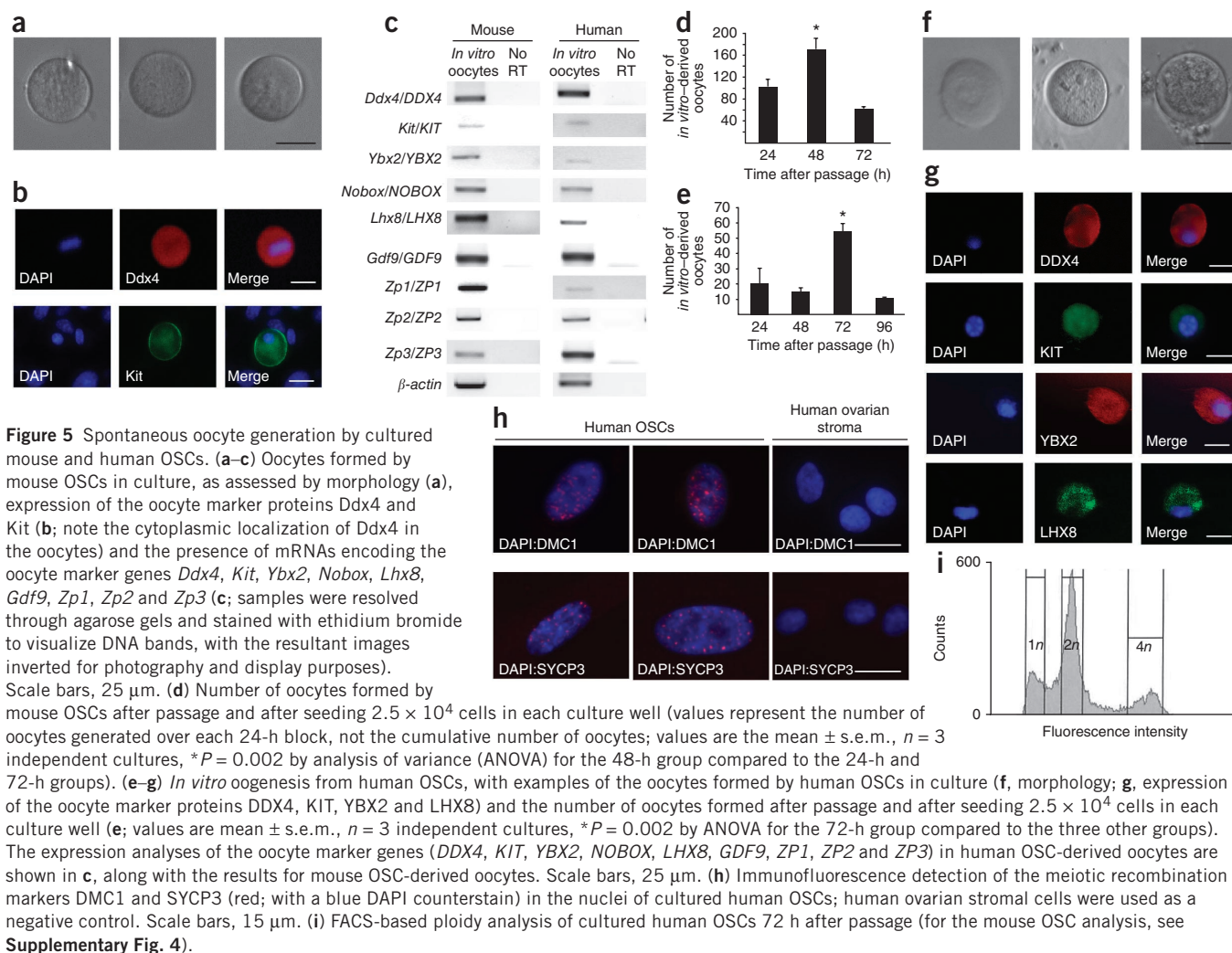
and the importance of these data will be highlighted in the next section. To extend the mRNA analyses of *Prdm1* and *PRDM1*, *Dppa3* and *DPPA3*, and *Ifitm3* and *IFITM3*, we performed an immunofluorescence analysis of these three classic primitive germline markers^{17,18}. We easily and uniformly detected all three proteins coded for by these marker genes in mouse (Fig. 4h) and human (Fig. 4i) OSCs maintained *in vitro*. Notably, our detection of *Ifitm3* and *IFITM3* in these cells agrees with a recent study reporting that this protein can also be used to isolate OSCs from mouse ovaries by immunomagnetic bead sorting²¹.

***In vitro* oogenic capacity of candidate human OSCs**

Consistent with results from others⁶, mouse OSCs cultured *in vitro* spontaneously generated large (35–50 μ m in diameter) spherical cells that, by morphology (Fig. 5a) and gene expression analyses (Fig. 5b,c), resembled oocytes. We observed the peak *in vitro* oogenesis from mouse OSCs within 24–48 h after each passage (Fig. 5d), which was followed by a progressive decline to nearly non-detectable amounts of oogenesis each time the OSCs regained confluence. A parallel analysis of DDX4-positive cells isolated from adult human ovaries and maintained *in vitro* revealed that these cells, like mouse OSCs, also spontaneously generated oocytes (Fig. 5e), as deduced from both morphological (Fig. 5f) and gene expression (Fig. 5c,g) analyses. The kinetics of *in-vitro* oogenesis from human OSCs differed slightly from mouse OSCs in that we observed the peak oocyte formation at 72 h after each passage in human OSC cultures (Fig. 5e), as compared to at 24–48 h in mouse OSC cultures (Fig. 5d). In addition to detection of many widely accepted oocyte markers (*Ddx4* and *DDX4*, *Kit* and *KIT* (the kit oncogene), *Nobox* and *NOBOX*, *Lhx8* and *LHX8* (LIM homeobox protein 8), *Gdf9* and *GDF9*, as well as *Zp1* and *ZP1*, *Zp2* and

ZP2, and *Zp3* and *ZP3* (zona pellucida glycoproteins 1–3)^{22–26}, mouse and human OSC-derived oocytes also expressed the diplotene-stage oocyte-specific marker *Ybx2* and *YBX2*, respectively (Y-box protein 2, also commonly referred to as *Msy2* or *MSY2* in mice and humans, respectively, as well as *CONTRIN* in humans) (Fig. 5c), which is essential for meiotic progression and gametogenesis in both sexes^{27,28}. Using adult human ovarian cortical tissue as a positive control, we identified four commercially available antibodies against oocyte markers that specifically reacted with the immature oocytes that are present in adult human ovaries (antibodies to DDX4, KIT, YBX2 and LHX8) (Supplementary Fig. 3); we also detected all four of these proteins in oocytes generated by human OSCs *in vitro* (Fig. 5g).

The presence of mRNA encoding the meiotic marker YBX2 in oocytes newly formed from human OSCs *in vitro* prompted us to next explore the prospects of meiotic entry in these cultures. An immunofluorescence analysis of human OSCs 72 h after passage identified cells with punctate nuclear localization of the meiosis-specific DNA recombinase dosage suppressor of mck1 homolog (DMC1) and the meiotic recombination protein synaptonemal complex protein 3 (SYCP3) (Fig. 5h). Both of these proteins are specific to germ cells and are necessary for meiotic recombination to proceed^{29–31}. Furthermore, an analysis of the chromosomal DNA content of human OSC cultures 72 h after passage revealed the presence of a diploid (2n) cell population; however, we also detected peaks corresponding to 4n and 1n cell



populations, the latter of which is indicative of germ cells that have reached haploid status³² (**Fig. 5i**). In the actively dividing cultures of human fibroblasts that we analyzed as controls in parallel, we detected only $2n$ and $4n$ populations of cells (**Supplementary Fig. 4a**). We also detected haploid ($1n$) cells in mouse OSC cultures after a FACS-based chromosomal analysis (**Supplementary Fig. 4b**).

Human OSCs generate oocytes in xenografted human ovary tissue

To confirm and extend the *in vitro* observations of oogenesis from candidate human OSCs, we stably transduced DDX4-positive cells isolated from adult human ovaries with a GFP expression vector (GFP-hOSCs) to facilitate cell tracking in two experiments. In the first experiment, we re-aggregated approximately 1×10^5 GFP-hOSCs with dispersed adult human ovarian cortical tissue. We observed numerous GFP-positive cells throughout the re-aggregated tissue (**Fig. 6a**). We then placed the aggregates in culture and assessed them 24–72 h later by direct (live-cell) GFP fluorescence. Within 24 h, several very large ($\geq 50 \mu$ m) single cells had formed within the aggregates, many of which were enclosed by smaller GFP-negative cells in tightly compact structures that resembled follicles; these structures remained detectable through 72 h of culture (**Fig. 6b,c**). We interpreted these findings as evidence that GFP-expressing human OSCs spontaneously generated oocytes that then became enclosed by somatic granulosa cells that were present in the adult human ovarian dispersates.

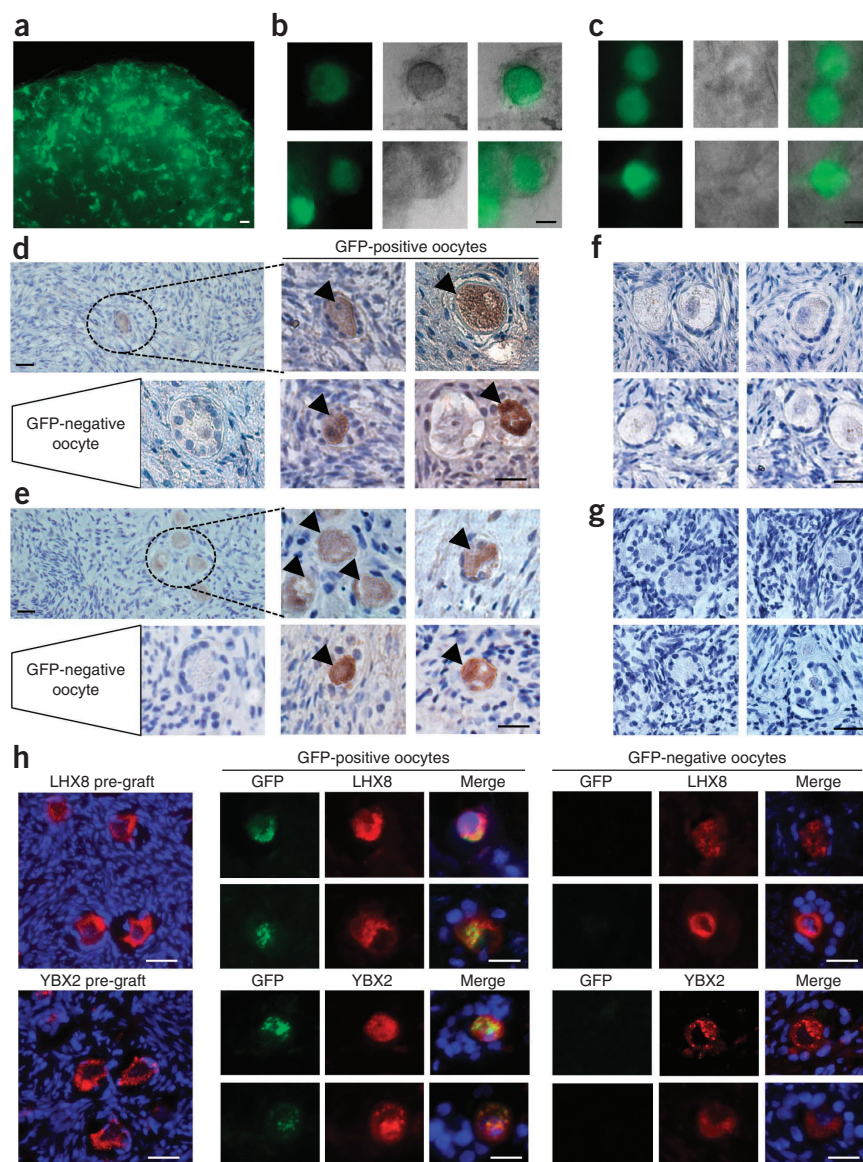
To more clearly determine whether this was indeed the case, we injected approximately 1.3×10^3 GFP-hOSCs into adult human ovarian cortical tissue biopsies ($2 \text{ mm} \times 2 \text{ mm} \times 1 \text{ mm}$), which we then xenografted into NOD-SCID female mice ($n = 40$ total grafts). We collected the grafts after 7 d or 14 d for assessment of GFP expression. All human ovary grafts contained easily discernible primordial and primary follicles with centrally located GFP-negative oocytes. Interspersed among and often adjacent to these follicles, which were presumably present in the tissue before the injection of the GFP-hOSCs, were other immature follicles containing GFP-positive oocytes (**Fig. 6d,e**). A serial-section histomorphometric analysis of three randomly selected human ovarian tissue grafts injected with GFP-hOSCs revealed the presence of 15–21 GFP-positive oocytes per graft 7 d after transplantation into mice (**Supplementary Fig. 5**). As controls, we used the human ovarian cortical tissue before the injection of GFP-hOSCs (**Fig. 6f**) or xenografts that received mock injections (vehicle without GFP-hOSCs) before transplantation into NOD-SCID mice (**Fig. 6g**). We never detected any GFP-positive oocytes in these controls. Dual-immunofluorescence-based detection of GFP, along with either the diplotene-stage oocyte-specific marker YBX2 or the oocyte-specific transcription factor LHX8, identified many GFP-YBX2 or GFP-LHX8 double-positive cells distributed throughout the xenografts that we injected with GFP-hOSCs (**Fig. 6h**). We detected no GFP-positive oocytes in human ovarian tissue before GFP-hOSC

Figure 6 Human OSCs generate oocytes in human ovary tissue. (**a–c**) Direct (live-cell) GFP fluorescence analysis of human ovarian cortical tissue after dispersion, re-aggregation with GFP-hOSCs (**a**) and *in vitro* culture for 24–72 h (**b,c**) showing the formation of large single GFP-positive cells surrounded by smaller GFP-negative cells in compact structures resembling follicles (scale bars, 50 μ m). (**d,e**) Immature follicles containing GFP-positive oocytes (brown, highlighted with black arrowheads, against a blue hematoxylin counterstain) in adult human ovarian cortical tissue injected with GFP-hOSCs and xenografted into NOD-SCID female mice (**d**, 1 week after transplant; **e**, 2 weeks after transplant). Examples of GFP-positive oocytes from multiple tissue replicates are shown. Scale bars, 25 μ m. There are comparable follicles with GFP-negative oocytes in the same grafts. (**f,g**) All immature follicles in human ovarian cortical tissue before GFP-hOSC injection and xenografting (**f**) or that received vehicle injection (no GFP-hOSCs) before xenografting (**g**) (negative controls) contained GFP-negative oocytes after processing for GFP detection in parallel with the samples shown. Scale bars, 25 μ m. (**h**) Dual immunofluorescence analysis of GFP expression (green) and either the diplotene-stage oocyte-specific marker YBX2 (red) or the oocyte transcription factor LHX8 (red) in xenografts receiving GFP-hOSC injections. Note that GFP was not detected in grafts before GFP-hOSC injection, whereas YBX2 and LHX8 were detected in all oocytes before and after injection. Sections were counterstained with DAPI (blue) for the visualization of nuclei. Scale bars, 25 μ m.

injection or in xenografts that did not receive GFP-hOSC injections (data not shown and **Fig. 6f,g**); however, the GFP-negative oocytes present in the tissue grafts were consistently positive for both YBX2 and LHX8 (**Fig. 6h** and **Supplementary Fig. 3**).

DISCUSSION

In 2004, a major paradigm shift in reproductive biology was proposed from a study in mice challenging the longstanding belief that ovaries of female mammals lose the capacity for oocyte generation before birth². Although this change in thinking was initially met with resistance from some members of the scientific community because of its sharp deviation from traditional beliefs in the field⁴, subsequent studies have since independently shown that mouse OSCs can be isolated from adult ovaries for long-term propagation *in vitro*^{5,6} and for generation of fertilization-competent eggs *in vivo* after intraovarian transplantation in chemotherapy-conditioned recipient female mice^{5,21}. In addition, other work has reported that *de novo* oocyte formation in adult mouse ovaries can be stimulated by small-molecule inhibitors of histone deacetylases, as well as by an as-yet unidentified factor(s) in the peripheral circulation of male mice^{7–9}. However, the potential clinical relevance of these findings with mice is unclear because of a lack of definitive evidence that ovaries of reproductive-age women contain a comparable population of oocyte-producing germline cells that match the characteristic features of mouse OSCs.



As a first step toward resolving this issue, we describe in detail the conceptual and technical validation of a straightforward and highly repeatable FACS-based approach for the purification of viable OSCs from adult mouse and human ovary tissue. The utility of an antibody directed against the C terminus of Ddx4 and DDX4 to isolate OSCs reflects a differentiation-dependent switch in localization of this protein in female germ cells from the cell surface (OSCs) to the cytoplasm (oocytes), with the latter being in accordance with traditional beliefs that Ddx4 and DDX4 are cytoplasmic proteins in germ cells in mice and humans, respectively. The physiological importance of this change in localization has not been determined; however, computer-based mapping of the Ddx4 and DDX4 transmembrane-spanning domain predicts that insertion of the C terminus of the protein across the cell membrane could potentially interfere with the RNA helicase domain^{10,33}. Although additional work will be needed to test this prediction, movement of proteins into and out of various cellular compartments is a post-translational mechanism that is commonly used by cells to regulate the activity of such proteins. We have incorporated this feature of Ddx4 and DDX4 into a FACS-based protocol to show that a rare population of mitotically active germ cells with

gene expression profiles and growth characteristics that are remarkably similar to mouse OSCs can be reliably isolated from ovaries of healthy young women and propagated long-term *in vitro*.

Our successful purification of what seems to be, by all criteria tested, the human equivalent of mouse OSCs was facilitated by two main factors: nearly 3 years of work in our laboratory to test and refine the protocol based on the use of antibodies to Ddx4 and DDX4 for isolation of OSCs using FACS rather than immunomagnetic sorting, as was reported initially⁵, and rare access to entire ovarian cortical tissues that had been vitrified and cryopreserved after the removal of both ovaries from women in their twenties and early thirties. Recent studies of mouse OSCs by others have showed the ability of these cells to generate immature oocytes *in vitro*⁶, as well as oocytes that mature into developmentally competent eggs *in vivo*⁵. Regarding the latter finding, it is notable that prior studies of mammalian germline stem cell transplantation using spermatogonial stem cells or OSCs have been performed with chemotherapy-conditioned hosts as recipients^{5,21,34,35}, presumably to open niches for effective donor-cell engraftment. Our observations show that for OSCs, adult female mice do not require chemotherapy conditioning before transplantation for these cells to effectively engraft in the ovaries and function long term (≥ 5 months), at least as measured by their ability to generate oocytes that mature in follicles that yield fertilization-competent eggs after ovulation. For ethical and legal reasons, as well as technical feasibility limitations related to a lack of validated protocols for efficiently maturing human primordial follicles to the antral stage *in vitro* for the isolation of metaphase-II oocytes, our current endpoint analysis of the equivalent cells in humans could not be as comprehensive. Nonetheless, we have established a consistent and close parallelism between human-ovary-derived DDX4-positive cells and mouse OSCs in terms of strategy of purification, yield from adult ovary tissue, morphology, primitive germline gene expression profile, *in vitro* growth properties, mitotic activity, meiotic activity and the ability to form oocytes in defined cultures *in vitro* and in injected ovary tissue *in vivo*.

Therefore, based on the multiple experimental lines of evidence reported herein, we feel it is reasonable to conclude that the rare cells with cell-surface expression of DDX4 that are present in the ovaries of reproductive-age women represent adult human OSCs. In addition to opening a new research field in human reproductive biology that was inconceivable less than 10 years ago, clear evidence for the existence of these cells in women may offer new opportunities to expand on and enhance current fertility-preservation strategies. For example, with assisted reproductive technologies involving cryopreservation of ovarian cortical tissue already in development for females with cancer^{36,37}, isolation and expansion of OSCs from this tissue before or after cryopreservation might be useful for new fertility applications. In fact, we found that these cells can be consistently obtained from cryopreserved and thawed human ovarian tissue samples, and that these cells *per se* can be cryopreserved and thawed months later with minimal loss for successful establishment *in vitro*. In addition, the availability of a detailed protocol for the purification of these newly discovered cells from human ovary tissue provides us and others with a much more physiologically relevant *in-vitro* model system from which to study human female germ cell development compared to the ESC-derived or induced pluripotent stem cell-derived germline cells that are currently used as models for human female gametogenesis^{38–42}.

METHODS

Methods and any associated references are available in the online version of the paper at <http://www.nature.com/naturemedicine/>.

Note: Supplementary information is available on the Nature Medicine website.

ACKNOWLEDGMENTS

The authors thank L. Prickett-Rice and K. Folz-Donahue of the Harvard Stem Cell Institute Flow Cytometry Core Facility and J. Groeneweg for expert technical assistance. We also thank J.R. Mann and K.J. MacLaughlin for the provision of TgOG2 transgenic mice. This work was supported by a Method to Extend Research in Time (MERIT) Award from the US National Institute on Aging (NIH R37-AG012279), the Henry and Vivian Rosenberg Philanthropic Fund, the Sea Breeze Foundation and Vincent Memorial Hospital Research Funds. This work was conducted while D.C.W. was supported in part by a Ruth L. Kirschstein National Research Service Award (NIH F32-AG034809).

AUTHOR CONTRIBUTIONS

Y.A.R.W., D.C.W. and J.L.T. designed the experiments, analyzed the data and wrote the manuscript. Y.A.R.W. and D.C.W. conducted the experiments. Y.T., O.I. and H.S. collected, cryopreserved and provided human ovarian cortical tissue. J.L.T. directed the project. All authors reviewed and approved the final manuscript for submission.

COMPETING FINANCIAL INTERESTS

The authors declare competing financial interests: details accompany the full-text HTML version of the paper at <http://www.nature.com/naturemedicine/>.

Published online at <http://www.nature.com/naturemedicine/>.

Reprints and permissions information is available online at <http://www.nature.com/reprints/index.html>.

1. Zuckerman, S. The number of oocytes in the mature ovary. *Recent Prog. Horm. Res.* **6**, 63–108 (1951).
2. Johnson, J., Canning, J., Kaneko, T., Pru, J.K. & Tilly, J.L. Germline stem cells and follicular renewal in the postnatal mammalian ovary. *Nature* **428**, 145–150 (2004).
3. Brinster, R.L. Male germline stem cells: from mice to men. *Science* **316**, 404–405 (2007).
4. Tilly, J.L., Niikura, Y. & Rueda, B.R. The current status of evidence for and against postnatal oogenesis in mammals: a case of ovarian optimism versus pessimism? *Biol. Reprod.* **80**, 2–12 (2009).
5. Zou, K. *et al.* Production of offspring from a germline stem cell line derived from neonatal ovaries. *Nat. Cell Biol.* **11**, 631–636 (2009).
6. Pacchiarotti, J. *et al.* Differentiation potential of germ line stem cells derived from the postnatal mouse ovary. *Differentiation* **79**, 159–170 (2010).
7. Johnson, J. *et al.* Oocyte generation in adult mammalian ovaries by putative germ cells in bone marrow and peripheral blood. *Cell* **122**, 303–315 (2005).
8. Wang, N. & Tilly, J.L. Epigenetic status determines germ cell meiotic commitment in embryonic and postnatal mammalian gonads. *Cell Cycle* **9**, 339–349 (2010).
9. Niikura, Y., Niikura, T., Wang, N., Satirapod, C. & Tilly, J.L. Systemic signals in aged males exert potent rejuvenating effects on the ovarian follicle reserve in mammalian females. *Aging* **2**, 999–1003 (2010).
10. Tilly, J.L. & Telfer, E.E. Purification of germline stem cells from adult mammalian ovaries: a step closer towards control of the female biological clock? *Mol. Hum. Reprod.* **15**, 393–398 (2009).
11. Niikura, Y., Niikura, T. & Tilly, J.L. Aged mouse ovaries possess rare premeiotic germ cells that can generate oocytes following transplantation into a young host environment. *Aging* **1**, 971–978 (2009).
12. Massasa, E., Costa, X.S. & Taylor, H.S. Failure of the stem cell niche rather than loss of oocyte stem cells in the aging ovary. *Aging* **2**, 1–2 (2010).
13. Fujiwara, Y. *et al.* Isolation of a DEAD-family protein gene that encodes a murine homolog of *Drosophila vasa* and its specific expression in germ cell lineage. *Proc. Natl. Acad. Sci. USA* **91**, 12258–12262 (1994).
14. Castrillon, D.H., Quade, B.J., Wang, T.Y., Quigley, C. & Crum, C.P. The human VASA gene is specifically expressed in the germ lineage. *Proc. Natl. Acad. Sci. USA* **97**, 9585–9590 (2000).
15. Noce, T., Okamoto-Ito, S. & Tsunekawa, N. Vasa homolog genes in mammalian germ cell development. *Cell Struct. Funct.* **26**, 131–136 (2001).
16. Normile, D. Reproductive biology. Study suggests a renewable source of eggs and stirs more controversy. *Science* **324**, 320 (2009).
17. Saitou, M., Barton, S.C. & Surani, M.A. A molecular programme for the specification of germ cell fate in mice. *Nature* **418**, 293–300 (2002).
18. Ohinata, Y. *et al.* Blimp1 is a critical determinant of the germ cell lineage in mice. *Nature* **436**, 207–213 (2005).
19. Dolci, S. *et al.* Stem cell factor activates telomerase in mouse mitotic spermatogonia and in primordial germ cells. *J. Cell Sci.* **115**, 1643–1649 (2002).
20. Gong, S.P. *et al.* Embryonic stem cell-like cells established by culture of adult ovarian cells in mice. *Fertil. Steril.* **93**, 2594–2601 (2010).
21. Zou, K., Hou, L., Sun, K., Xie, W. & Wu, J. Improved efficiency of female germline stem cell purification using Fragilis-based magnetic bead sorting. *Stem Cells Dev.* **20**, 2197–2204 (2011).

22. Suzumori, N., Yan, C., Matzuk, M.M. & Rajkovic, A. *Nobox* is a homeobox-encoding gene preferentially expressed in primordial and growing oocytes. *Mech. Dev.* **111**, 137–141 (2002).
23. Rajkovic, A., Pangas, S.A., Ballow, D., Suzumori, N. & Matzuk, M.M. NOBOX deficiency disrupts early folliculogenesis and oocyte-specific gene expression. *Science* **305**, 1157–1159 (2004).
24. Pangas, S.A. *et al.* Oogenesis requires germ cell-specific transcriptional regulators *Sohlh1* and *Lhx8*. *Proc. Natl. Acad. Sci. USA* **103**, 8090–8095 (2006).
25. Elvin, J.A., Clark, A.T., Wang, P., Wolfman, N.M. & Matzuk, M.M. Paracrine actions of growth differentiation factor-9 in the mammalian ovary. *Mol. Endocrinol.* **13**, 1035–1048 (1999).
26. Zheng, P. & Dean, J. Oocyte-specific genes affect folliculogenesis, fertilization, and early development. *Semin. Reprod. Med.* **25**, 243–251 (2007).
27. Gu, W. *et al.* Mammalian male and female germ cells express a germ cell-specific Y-Box protein, MSY2. *Biol. Reprod.* **59**, 1266–1274 (1998).
28. Yang, J. *et al.* Absence of the DNA/RNA-binding protein MSY2 results in male and female infertility. *Proc. Natl. Acad. Sci. USA* **102**, 5755–5760 (2005).
29. Page, S.L. & Hawley, R.S. The genetics and molecular biology of the synaptonemal complex. *Annu. Rev. Cell Dev. Biol.* **20**, 525–558 (2004).
30. Yuan, L. *et al.* Female germ cell aneuploidy and embryo death in mice lacking the meiosis-specific protein SCP3. *Science* **296**, 1115–1118 (2002).
31. Kagawa, W. & Kurumizaka, H. From meiosis to postmeiotic events: uncovering the molecular roles of the meiosis-specific recombinase *Dmc1*. *FEBS J.* **277**, 590–598 (2010).
32. West, F.D., Mumaw, J.L., Gallegos-Cardenas, A., Young, A. & Stice, S.L. Human haploid cells differentiated from meiotic competent clonal germ cell lines that originated from embryonic stem cells. *Stem Cells Dev.* **20**, 1079–1088 (2011).
33. Abban, G. & Johnson, J. Stem cell support of oogenesis in the human. *Hum. Reprod.* **24**, 2974–2978 (2009).
34. Brinster, R.L. & Zimmermann, J.W. Spermatogenesis following male germ-cell transplantation. *Proc. Natl. Acad. Sci. USA* **91**, 11298–11302 (1994).
35. Brinster, C.J. *et al.* Restoration of fertility by germ cell transplantation requires effective recipient preparation. *Biol. Reprod.* **69**, 412–420 (2003).
36. Oktay, K. & Karlikaya, G. Ovarian function after transplantation of frozen, banked autologous ovarian tissue. *N. Engl. J. Med.* **342**, 1919 (2000).
37. Sönmezer, M. & Oktay, K. Orthotopic and heterotopic ovarian tissue transplantation. *Best Pract. Res. Clin. Obstet. Gynaecol.* **24**, 113–126 (2010).
38. Hübner, K. *et al.* Derivation of oocytes from mouse embryonic stem cells. *Science* **300**, 1251–1256 (2003).
39. Ko, K. & Schöler, H.R. Embryonic stem cells as a potential source of gametes. *Semin. Reprod. Med.* **24**, 322–329 (2006).
40. Nicholas, C.R., Haston, K.M., Grewall, A.K., Longacre, T.A. & Reijo Pera, R.A. Transplantation directs oocyte maturation from embryonic stem cells and provides a therapeutic strategy for female infertility. *Hum. Mol. Genet.* **18**, 4376–4389 (2009).
41. Kee, K., Angeles, V.T., Flores, M., Nguyen, H.N. & Reijo Pera, R.A. Human *DAZL*, *DAZ* and *BOULE* genes modulate primordial germ-cell and haploid gamete formation. *Nature* **462**, 222–225 (2009).
42. Nicholas, C.R., Chavez, S.L., Baker, V.L. & Reijo Pera, R.A. Instructing an embryonic stem cell-derived oocyte fate: lessons from endogenous oogenesis. *Endocr. Rev.* **30**, 264–283 (2009).

ONLINE METHODS

Mice. Wild-type C57BL/6 and NOD-SCID mice were from Charles River Laboratories and Jackson Laboratories, respectively. Transgenic mice with germline-specific GFP expression (TgOG2)^{43–45} were obtained, bred and genotyped as described^{7,46}. All animal protocols were reviewed and approved by the institutional care and use committee of Massachusetts General Hospital.

Human samples. After obtaining written informed consent, ovaries were surgically removed from six female subjects between 22 and 33 years of age with gender identity disorder who were receiving sex reassignment at Saitama Medical Center. The outer cortical layer of each ovary was carefully removed, vitrified and cryopreserved⁴⁷. For our experiments, the cryopreserved tissue was thawed using the Cryotissue Thawing Kit (KITAZATO BioPharma). All experiments with human tissue were conducted without subject identifiers under a protocol reviewed and approved by the institutional review board of Massachusetts General Hospital (protocol number 2008P001640).

DDX4 antibodies. Polyclonal antibodies against the C (ab13840; Abcam) or N (AF2030; R&D Systems) terminus of DDX4 were from Abcam or R&D Systems, respectively.

Immunomagnetic sorting. Dissociated ovarian cells or isolated oocytes were processed by immunomagnetic sorting using streptavidin-conjugated microbeads (Miltenyi) or secondary-antibody-conjugated Dynabeads (Invitrogen), as described⁵.

Flow cytometry. Antibody-labeled ovarian cell suspensions were subjected to FACS using a BD Biosciences FACSARIA II cytometer (Harvard Stem Cell Institute) gated against negative controls (unstained cells and cell fractions processed without primary antibody).

Teratoma formation. Mouse ESCs (mESC v6.5) or freshly isolated mouse OSCs were injected subcutaneously near the rear haunch of NOD-SCID female mice, which were then monitored weekly for up to 6 months after injection for tumor formation.

OSC cultures. Mouse and human OSCs were established on mitotically inactivated immortalized MEFs and propagated *in vitro*, essentially as described⁵. To assess OSC proliferation, MEF-free OSC cultures were treated with 10 μ M BrdU (Sigma-Aldrich) for 48 h for dual-immunofluorescence-based detection of BrdU incorporation and Ddx4 or DDX4 expression, essentially as described⁵.

Gene expression. The presence of each indicated mRNA was assessed by conventional RT-PCR using the primers listed in **Supplementary Tables 1** (mouse) and **2** (human).

Immunoanalyses. Fixed ovarian tissues, OSCs or oocytes were assessed by standard immunohistochemical or immunocytochemical methods using antibodies that recognize Ddx4 and DDX4 (C terminus: ab13840, Abcam; N terminus: AF2030, R&D Systems), Kit and KIT (sc1494, Santa Cruz Biotechnology), Prdm1 and PRDM1 (ab81961, Abcam), Dppa3 and DPPA3 (ab19878, Abcam), Ifitm3 and IFITM3 (mouse: ab15592, human: ab74699, Abcam), DMC1 (ab96613, Abcam), SYCP3 (NB300-232, NOVUS Biologicals), YBX2 (ab33164, Abcam) or LHX8 (ab41519, Abcam).

Ploidy analysis. A chromosomal analysis of mouse and human OSCs was performed using a BD Biosciences FACSARIA II cytometer, essentially as described³². Human fetal kidney fibroblasts (KEK 293, Invitrogen) were used as control somatic cells.

Generation of GFP-expressing OSCs. One microgram of *pBabe-Gfp* vector DNA (Addgene plasmid repository #10668) was transfected (Lipofectamine, Invitrogen) into the Platinum-A retroviral packaging cell line (Cell Biolabs). Transduction of OSCs was performed using fresh viral supernatant in the presence of polybrene (Sigma-Aldrich). Mouse and human OSCs with expression of GFP were purified by FACS after an initial 1 week of propagation and then were expanded for 2 additional weeks before a second round of FACS purification to obtain the cells used for the experiments.

Transplantation of mouse OSCs. GFP-expressing mouse OSCs (1×10^4) were injected directly into each ovary of wild-type mice at 2 months of age. Between 7 and 8 months of age, the mice were subjected to an induced ovulation protocol. Cumulus-oocyte complexes were collected from the oviducts and assessed by direct fluorescence microscopy for GFP expression. For IVF, cumulus-oocyte complexes were mixed with wild-type sperm for 4–5 h, washed and transferred to potassium simplex optimized medium with amino acids (Irvine Scientific). Light and fluorescence microscopic examinations were performed every 24 h for a total of 144 h to monitor embryo development⁴⁸. Ovarian tissue harvested at the time of oocyte collection was processed for immunohistochemical detection of GFP, as detailed⁴⁶.

Human ovarian tissue re-aggregation. Dissociated human ovarian cortex was incubated with 35 μ g ml⁻¹ phytohemagglutinin (PHA; Sigma), along with 1×10^5 GFP-expressing human OSCs for 10 min at 37 °C. The cell mix was pelleted to create the tissue aggregate, which was then placed onto a Millicell 0.4- μ m culture plate insert (Millipore) in OSC culture medium. Aggregates were incubated at 37 °C in 5% CO₂ and 95% air, and live-cell GFP imaging was performed 24, 48 and 72 h later.

Intraovarian OSC injection and xenografting. Human ovarian cortical tissue injected with approximately 1.3×10^3 GFP-expressing human OSCs was grafted into NOD-SCID female mice^{49,50}. Xenografts were removed 7 d or 14 d after transplantation and were processed for immunohistochemical detection of GFP expression⁴⁶. For the dual marker analysis, we performed immunofluorescence-based detection of GFP and either YBX2 or LHX8 (see above).

Data analyses. All experiments were independently replicated at least three times. Quantitative data (means \pm s.e.m. of combined results) were analyzed by one-way ANOVA using Prism software, whereas the qualitative images presented are representative of outcomes obtained in replicate experiments.

Additional methods. Detailed methodology is described in the **Supplementary Methods**.

43. Yeom, Y.I. *et al.* Germline regulatory element of Oct-4 specific for the totipotent cycle of embryonal cells. *Development* **122**, 881–894 (1996).
44. Yoshimizu, T. *et al.* Germline-specific expression of the Oct-4/green fluorescent protein (GFP) transgene in mice. *Dev. Growth Differ.* **41**, 675–684 (1999).
45. Szabó, P.E. *et al.* Allele specific expression of imprinted genes in mouse migratory primordial germ cells. *Mech. Dev.* **115**, 157–160 (2002).
46. Lee, H.-J. *et al.* Bone marrow transplantation generates immature oocytes and rescues long-term fertility in a preclinical mouse model of chemotherapy-induced premature ovarian failure. *J. Clin. Oncol.* **25**, 3198–3204 (2007).
47. Kagawa, N., Silber, S. & Kuwayama, M. Successful vitrification of bovine and human ovarian tissue. *Reprod. Biomed. Online* **18**, 568–577 (2009).
48. Selesniemi, K., Lee, H.-J., Muhlhäuser, A. & Tilly, J.L. Prevention of maternal aging-associated oocyte aneuploidy and meiotic spindle defects in mice by dietary and genetic strategies. *Proc. Natl. Acad. Sci. USA* **108**, 12319–12324 (2011).
49. Weissman, A. *et al.* Preliminary experience with subcutaneous human ovarian cortex transplantation in the NOD-SCID mouse. *Biol. Reprod.* **60**, 1462–1467 (1999).
50. Matikainen, T. *et al.* Aromatic hydrocarbon receptor-driven *Bax* gene expression is required for premature ovarian failure caused by biohazardous environmental chemicals. *Nat. Genet.* **28**, 355–360 (2001).